

On the role of oxygen in dielectric barrier discharge actuation of aerodynamic flows

Cite as: Appl. Phys. Lett. **91**, 181501 (2007); <https://doi.org/10.1063/1.2803755>

Submitted: 12 September 2007 . Accepted: 08 October 2007 . Published Online: 29 October 2007

W. Kim, H. Do, M. G. Mungal, and M. A. Cappelli



View Online



Export Citation

ARTICLES YOU MAY BE INTERESTED IN

[Contribution of positive and negative ions to the electrohydrodynamic force in a dielectric barrier discharge plasma actuator operating in air](#)

Journal of Applied Physics **106**, 023115 (2009); <https://doi.org/10.1063/1.3183960>

[Time-correlated force production measurements of the dielectric barrier discharge plasma aerodynamic actuator](#)

Journal of Applied Physics **103**, 073302 (2008); <https://doi.org/10.1063/1.2896590>

[Modeling of dielectric barrier discharge plasma actuator in air](#)

Journal of Applied Physics **103**, 053305 (2008); <https://doi.org/10.1063/1.2837890>



Your Qubits. Measured.

Meet the next generation of quantum analyzers

- Readout for up to 64 qubits
- Operation at up to 8.5 GHz, mixer-calibration-free
- Signal optimization with minimal latency

[Find out more](#)



Zurich
Instruments

On the role of oxygen in dielectric barrier discharge actuation of aerodynamic flows

W. Kim,^{a)} H. Do, M. G. Mungal, and M. A. Cappelli

Mechanical Engineering Department, Stanford University, Stanford, California 94305-3032

(Received 12 September 2007; accepted 8 October 2007; published online 29 October 2007)

Phase-locked particle image velocimetry is used to study the mechanism of induced flow in the near field of a rf dielectric barrier discharge actuator mounted in the separated flow region of a bluff body. Flow actuation is found to be asymmetric, with suction toward the buried downstream electrode when it is biased positively relative to the upstream exposed electrode. Lesser flow is seen on the reverse voltage swing, where the buried electrode should attract positive ions. This phenomenon is enhanced when oxygen is added to the flow, suggesting that oxygen negative ions, possibly O_2^- , play a dominant role in plasma actuation. © 2007 American Institute of Physics.

[DOI: 10.1063/1.2803755]

Plasma-based methods of aerodynamic flow control have emerged over the past decade. One method employs surface-embedded dielectric barrier discharge (DBD) actuators,^{1–5} in which radio frequency (rf)-induced ion migration (“ion wind”) imparts momentum transfer to near-surface fluid, generating a wall jet that alters the boundary layer properties. This surface actuation has been used to control flow separation and thereby reduce aerodynamic drag,⁶ or alter lift on air foils at high angle of attack.⁷

The DBD actuator is a simple device, a schematic of which is shown in Fig. 1, on the bluff body studied here. The reader is directed to the thorough review of these and other types of plasma actuators by Moreau⁸ for more details, as only a brief account of its operation is presented here. Layered on top of the aerodynamic surface, the actuator consists of buried and exposed thin conducting electrodes separated by a dielectric material (e.g., polycarbonate foil), driven at rf voltages (~ 5 – 10 kV) at frequencies ranging from 1 to 30 kHz. Conventional wisdom related to the operation of these discharges, based on numerical simulations,^{9,10} is that the electrons generated by avalanche ionization near the exposed electrode during the forward stroke of the rf cycle (when the exposed electrode is driven negative relative to the buried electrode) rapidly migrate toward the dielectric barrier and accumulate on its surface. Positive ions generated during this forward stroke migrate toward and recombine on the exposed electrode. The rapid electron migration and charge accumulation self-terminate this discharge. During the reverse stroke, the electrons are quickly discharged from the dielectric surface, stream toward the exposed electrode, and further participate in avalanche ionization, eventually recombining on the exposed electrode. While a single streamer event can last tens of nanoseconds in duration, multiple streamers can take place over the entire electrode, resulting in nanosecond pulse bursts of current during this forward stroke. The positive ions born during this phase of the cycle migrate toward the buried electrode, producing strong ion wind suction through momentum exchange collisions with background neutrals. The plasma density during this reverse stroke is calculated to be larger than that of the forward stroke, due to the electron streaming and subsequent ioniza-

tion from the stored surface charge on the dielectric.¹⁰ As a result, the computed force on the neutral fluid due to the positive ion migration generated during the reverse stroke is calculated to be much greater than that of the reverse positive ion migration on the forward stroke, and the result is a net force in the direction away from the exposed electrode, generating a so-called wall jet.⁸

Recent experiments¹¹ indicate that the strength of the actuation of the flow is greater in flows containing oxygen in comparison to those in pure nitrogen, suggesting that oxygen ions (possibly even negative ions) play a significant role in the force mechanism. It is not surprising that copious levels of oxygen negative ions can be generated in these discharges, since other types of reactive oxygen were found to be important in the application of similar discharges to sterilization.¹² Numerical simulations¹⁰ confirm that the total ion concentrations in pure O_2 are more abundant than in pure N_2 during the reverse stroke of the DBD discharge—a result attributed to the lower ionization potential of O_2 .¹⁰ These and other simulations¹³ included the formation of O^- ions, which were found to have only a slight effect of diminishing the force during the reverse stroke.

In this letter, we provide compelling evidence that the greatest suction force with DBD actuation is generated during the *forward stroke* of the discharge, contrary to conven-

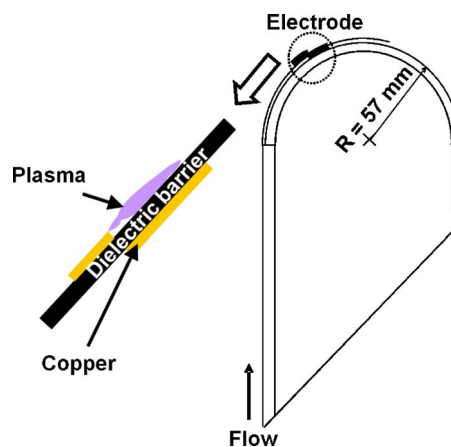


FIG. 1. (Color online) Schematic of DBD plasma actuator positioned on a bluff body on a flow. A close-up of the electrode pair is shown to the left.

^{a)}Electronic mail: wkim@stanford.edu

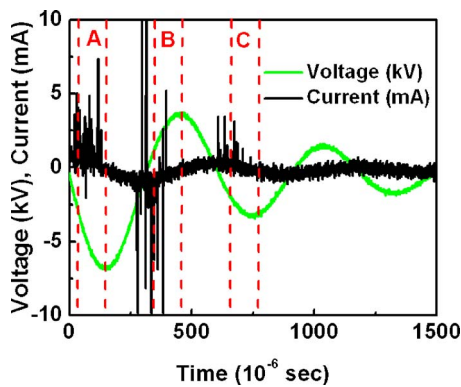


FIG. 2. (Color online) Voltage excitation waveform and discharge current. The vertical markers represent the first and second laser pulses for PIV imaging, and three phase-locked locations within the waveform.

tional wisdom. Paraelectric¹⁴ forces alone do not satisfactorily account for this asymmetry between the forward and reverse strokes of the rf cycle. One possible explanation for this asymmetric behavior is the formation of negative ions during the forward stroke, most likely O_2^- , that migrate toward the dielectric to cause this suction flow. Surprisingly, we see little flow during the reverse stroke, suggesting that electrons released from the dielectric gain too much energy to favor electron attachment (the attachment coefficient diminishes with increased field¹⁵), and possibly form positive ions that generate a weaker suction flow.

The measurements are carried out in the near field of a single electrode-pair actuator integrated into the surface of a bluff body exposed to a 0.7 m/s air flow in a wind tunnel, as seen in Fig. 1. The DBD used here consists of 90 μm thick copper electrode foil between which is a 520 μm thick glass fiber dielectric tape. The exposed electrode is upstream of that buried below the dielectric layer. This particular aerodynamic flow configuration is intended to simulate the DBD plasma-induced turning of an otherwise separated air stream following the formation of relatively thick boundary layers.¹⁶ The boundary layer is generated by connecting a 200 mm long flat plate to the tangent of a 114 mm diameter half-cylinder, with the flat plate oriented parallel to the free stream. For the results described here, the single electrode pair is placed on the bluff body at an angle of 60° from where the flat plate contacts the half cylinder, where separation is seen at these flow conditions. In our past studies,¹⁶ multiple actuator pairs were distributed over the cylinder to achieve stronger actuation, and the electrodes were driven by periodic rf voltages. In the study presented here, we use a single electrode pair to simplify the interpretation of the resulting actuated flow, since we found that significant electrode-pair interactions exist when multiple electrode pairs are placed around the cylinder. Furthermore, we use, instead of steady rf actuation, a power supply capable of producing a burst of at most two (11 kV peak-to-peak voltage) rf cycles, at a repetition rate of 260 Hz. Typical voltage (of the exposed electrode relative to the buried electrode) and current (measured at the buried electrode) traces are shown in Fig. 2. During flow actuation, the luminous discharge extends 3 mm in the streamwise direction above the buried electrode and is approximately 20 mm wide in the direction of gas flow.

Phase-locked particle Image Velocimetry (PIV) is used to measure the local instantaneous flow velocity at specific

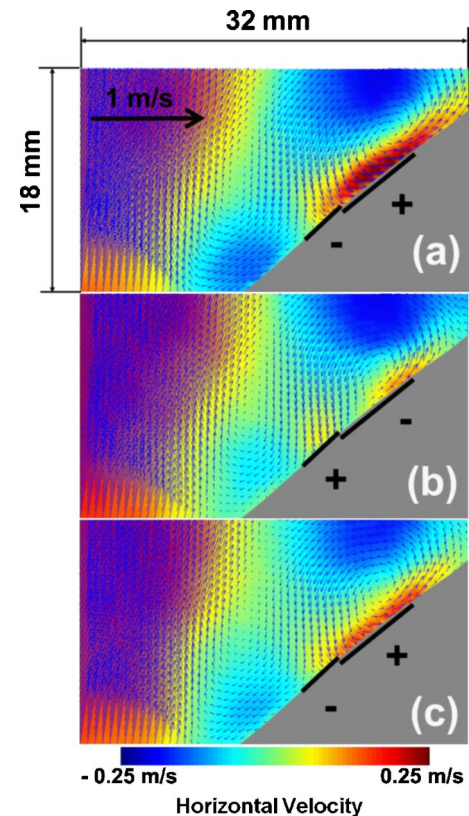


FIG. 3. (Color online) PIV images of velocity in the near field of a DBD plasma actuator: (a) forward stroke of the dominant rf cycle, (b) backward stroke, and (c) forward stroke of the second, weaker rf cycle. Red color represents strong components of velocity toward the right, and blue represents flow velocity to the left.

times within the voltage cycle. Phase-locked PIV is widely used in experimental fluid mechanics and was used recently to study the dynamics of DBD-driven synthetic plasma jets.¹⁷ PIV involves the collection of Mie scattering images of particles (here, 0.3 μm nominal diameter alumina) seeded into the flow from successively pulsed laser sheets. A cross-correlation analysis of the particle positions in the two images is used to extract the velocity over the time between the laser pulses. Figure 2 also depicts the three time intervals (labeled A, B, and C) within the voltage cycle over which the flow velocity field is captured by PIV. The two consecutive 532 nm laser sheets used to illuminate the flow are separated by 120 μs . Electrophoretic forces are found to be negligible, through a controlled experiment comparing the seed particle density distributions in the absence and presence of the discharge.

Velocity fields obtained from an ensemble average of 100 instantaneous PIV images phase-locked to regions A, B, and C are shown in Figs. 3(a)–3(c), respectively. Note that in these figures, which encompass a close-up of the near-field region of the actuator on the cylinder, the direction of free stream air is from the bottom to the top, and the red color coding represents a region which has high (suction) flow to the right while blue color coding shows a region which has high velocity component to the left. The gray region and black stripes serve to illustrate the locations of the body and electrode pairs, respectively.

We see that when the exposed electrode is negatively biased relative to the buried electrode, i.e., during the forward stroke of the first rf cycle [Fig. 3(a)], there is a signifi-

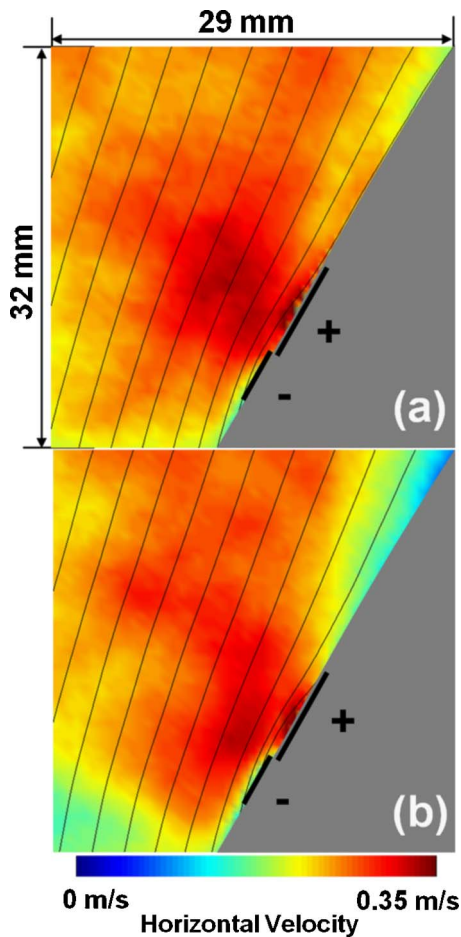


FIG. 4. (Color online) Ensemble-average PIV images of the velocity field for oxygen-enriched flow (top) and nitrogen-enriched flow (bottom). Black solid lines represent pseudostreamlines released in the flow. In this particular case, the electrode pair is placed on the bluff body at an angle of 30° along the half-cylinder.

cant suction flow into the buried electrode. This provides compelling evidence that negatively charged ions are created during this phase of the cycle and migrate toward the dielectric surface. When the applied field reverses [Fig. 3(b)], making the buried electrode more negative with respect to the exposed electrode, the strong suction diminishes but is not eliminated, as evidenced by the yellow shading in the immediate vicinity of the surface. We believe that this weaker flow is driven by a lesser degree of positive ion migration. During the first phase of the second, weaker cycle [Fig. 3(c)], the suction flow returns, although it is not as strong as that in Fig. 3(a), since the applied voltage is correspondingly lower. Flow effects diminish rapidly as the rf pulses become weaker in intensity.

To confirm that the source of the suction flow is attributable to oxygen species, experiments were conducted in oxygen enriched air (31% oxygen by volume) and in nitrogen enriched air (83% nitrogen by volume). The strength of the suction flow is found to be correspondingly stronger in oxygen-rich cases, and weaker in nitrogen-rich cases, as can be seen from the ensemble-averaged PIV images in Fig. 4. This supports the findings in the experiments presented in Ref. 11 but further clarifies the force mechanism. Our data present evidence that oxygen and *oxygen negative ions*, in particular, are responsible for the majority of the actuation force when these DBD plasmas are operated in air, and that the force is generated predominantly during the *forward stroke* of the rf cycle when the dielectric surface is attracting negative charge.

This work was sponsored by the AFOSR/MURI Program—Experimental/Computational Studies of Combined-Cycle Propulsion: Physics and Transient Phenomena in Inlets and Scramjet Combustors, a joint effort of the University of Texas at Austin and Stanford University, with Julian Tishkoff as Technical Monitor.

¹J. R. Roth, D. M. Sherman, and S. P. Wilkinson, 36th AIAA Aerospace Sciences Meeting and Exhibition, Reno, NU, 1998 (unpublished), Paper No. 1998-0328.

²J. R. Roth, D. M. Sherman, and S. P. Wilkinson, AIAA J. **38**, 1172 (2000).

³J. R. Roth, Phys. Plasmas **10**, 2117 (2003).

⁴C. L. Enloe, T. E. McLaughlin, R. D. Van Dyken, K. D. Kachner, E. J. Jumper, T. C. Corke, M. Post, and O. Haddad, AIAA J. **42**, 595 (2004).

⁵C. L. Enloe, T. E. McLaughlin, R. D. Van Dyken, and K. D. Kachner, AIAA J. **42**, 589 (2004).

⁶Y. Sung, W. Kim, M. G. Mungal, and M. A. Cappelli, Exp. Fluids **41**, 479 (2006).

⁷M. L. Post and T. C. Corke, 41st AIAA Aerospace Sciences Meeting and Exhibition, Reno, NU, 2003 (unpublished), Paper No. 2003-1024.

⁸E. Moreau, J. Phys. D **40**, 605 (2007).

⁹J. P. Boeuf, Y. Lagmich, Th. Unter, Th. Callegari, and L. C. Pitchford, J. Phys. D **40**, 652 (2007).

¹⁰G. I. Font and W. L. Morgan, Contrib. Plasma Phys. **47**, 103 (2007).

¹¹C. L. Enloe, T. E. McLaughlin, G. I. Font, and J. W. Baughn, 43rd Aerospace Sciences Meeting and Exhibition, Reno, NU, 2005 (unpublished), Paper No. 2005-0564.

¹²T. C. Montie, K. Kelly-Wintenberg, and J. R. Roth, IEEE Trans. Plasma Sci. **28**, 41 (2000).

¹³K. P. Singh and S. Roy, J. Appl. Phys. **101**, 123308 (2007).

¹⁴J. R. Roth, *Industrial Plasma Engineering Volume II—Applications to Non-Thermal Plasma Processing* (Institute of Physics, Bristol, 2001), 2, 225.

¹⁵J. Dutton, F. Llewellyn-Jones, and G. B. Morgan, Nature (London) **198**, 680 (1963).

¹⁶H. Do, W. Kim, M. G. Mungal, and M. A. Cappelli, 45th AIAA Aerospace Sciences Meeting and Exhibition, Reno, NU, 2007 (unpublished), Paper No. 2007-939.

¹⁷A. Santhanakrishnan and J. D. Jacob, J. Phys. D **40**, 637 (2007).